JPPIPA 11(12) (2025)

Jurnal Penelitian Pendidikan IPA

http://jppipa.unram.ac.id/index.php/jppipa/index

High-Resolution Thermal Mapping for Urban Heat Mitigation: Random Forest Downscaling in a Rapid Urbanization Context (Case Study Malang City, Indonesia)

Nevy Ardianto[1*], Aminudin Afandhi[2], Abu Bakar Sambah[3]

[1] Postgraduate School, University of Brawijaya, Malang, Indonesia.
[2] Faculty of Agriculture, University of Brawijaya, Malang, Indonesia.
[3] Faculty of Fisheries and Marine Sciences, University of Brawijaya, Malang, Indonesia.

Received: October 07, 2025
Revised: November 14, 2025
Accepted: December 25, 2025
Published: December 31, 2025

Corresponding Author:
Nevy Ardianto
nevyardianto@student.ub.ac.id

DOI: 10.29303/jppipa.v11i12.13393

© 2025 The Authors. This open access article is distributed under a (CC-BY License)

Abstract: This study aims to enhance the spatial resolution of land surface temperature (LST) mapping in Malang City, Indonesia, and to analyze spatiotemporal urban thermal dynamics associated with rapid urbanization. Landsat 8 OLI/TIRS thermal data were integrated with Sentinel-2 multispectral imagery using a Random Forest (RF)–based downscaling approach to refine LST resolution from 30 m to 10 m. Spectral indices, including NDVI, NDBI, NDWI, and NDMI, were employed as predictor variables, and model performance was evaluated using R^2 and RMSE metrics, supported by in-situ temperature measurements for validation. The results demonstrate strong downscaling performance, with R^2 values of 0.8374 (2019), 0.8468 (2022), and 0.7675 (2024), while field validation yielded a correlation coefficient of 0.722 and an RMSE of 4.63°C. Spatial and temporal analyses reveal a significant increase in mean LST from 24.67°C in 2019 to 27.21°C in 2024, indicating accelerated urban warming, particularly during 2022–2024. This warming is closely associated with land-use transformation, increased impervious surfaces, and regional climatic influences. In conclusion, the RF-based downscaling approach effectively captures fine-scale urban thermal heterogeneity and provides reliable high-resolution LST information, supporting urban heat mitigation planning and climate adaptation strategies in rapidly growing tropical cities.

Keywords: Downscaling; Land surface temperature; Landsat-8; Random forest; Remote sensing; Sentinel-2

Introduction

Malang City, located in East Java, Indonesia, is one of the region's rapidly urbanizing centres, experiencing substantial land-use and land-cover (LULC) transformations over the past two decades (Hasyim et al., 2025). The city's transition from a mid-sized highland settlement to a major urban centre has been accompanied by extensive conversion of agricultural lands and vegetated areas into residential, commercial, and transportation infrastructure (Hasyim et al., 2025). These landscape modifications have fundamentally altered the city's natural thermal characteristics by reducing vegetation-mediated cooling capacity and increasing thermal energy accumulation in built-up zones (Voogt & Oke, 2003).

Rapid urbanization in Malang City has been driven by population growth, with the city recording 889.359 inhabitants in 2024 and an annual population growth rate of 0.5% (Isdianto et al., 2025). This demographic pressure intensifies LULC conversion processes, leading to the proliferation of impervious materials such as asphalt and concrete that absorb and re-emit substantial quantities of solar radiation (Santamouris, 2020). These materials exhibit lower surface reflectivity (albedo) than natural land covers, thereby enhancing thermal energy retention and contributing to the pronounced Urban Heat Island (UHI) effect (Santamouris, 2020). The UHI

How to Cite:
Ardianto, N., Afandhi, A., & Sambah, A. B. (2025). High-Resolution Thermal Mapping for Urban Heat Mitigation: Random Forest Downscaling in a Rapid Urbanization Context (Case Study Malang City, Indonesia). *Jurnal Penelitian Pendidikan IPA*, *11*(12), 1390-1401. https://doi.org/10.29303/jppipa.v11i12.13393

phenomenon presents a significant environmental challenge, particularly in tropical urban environments, as it elevates local surface and air temperatures, disrupts microclimatic equilibrium, and compromises urban livability and public health (Irfeey et al., 2023).

Alterations in land surface characteristics directly influence the dynamics of the energy balance among radiation, convection, and evaporation, which determine LST (Li et al., 2024). LST serves as a critical biophysical indicator for assessing surface thermal properties and understanding the spatial distribution of urban thermal anomalies (Voogt & Oke, 2003). Elevated LST values in urban areas are consistently associated with reduced vegetation coverage, increased building density, and extensive impervious surface distribution, which extend thermal retention periods relative to natural land covers (Isdianto et al., 2025).

Continuous monitoring of LST variations is essential for quantifying urban thermal stress and developing evidence-based adaptive planning strategies to mitigate climate-related risks and enhance urban resilience. However, the spatial resolution limitations of operational thermal satellite data impose significant constraints on the accuracy of temperature mapping in heterogeneous urban environments. Landsat 8 thermal infrared observations, for example, provide LST data at 100 m resolution (commonly resampled to 30 m), which proves inadequate for detailed urban-scale thermal analysis (Onačillová et al., 2022). While this resolution may be appropriate for regional-scale assessments, it fails to capture microscale thermal variations such as temperature gradients between individual roads, building complexes, and small urban vegetation patches.

Sentinel-2, operated by the European Space Agency (ESA), delivers multispectral imagery at 10–20 m spatial resolution but lacks thermal infrared observations. Nevertheless, Sentinel-2's high-resolution spectral information, particularly in visible and shortwave infrared bands, provides valuable ancillary data for deriving spectral indices, including Normalized Difference Vegetation Index (NDVI), Normalized Difference Built-up Index (NDBI), Normalized Difference Water Index (NDWI), and Normalized Difference Moisture Index (NDMI), which exhibit strong correlations with surface temperature. The integration of Sentinel-2 spectral data with Landsat thermal data offers a viable approach to overcoming spatial resolution constraints through statistical or algorithmic downscaling.

Downscaling encompasses statistical and computational techniques that enhance the spatial resolution of coarse datasets by integrating them with higher-resolution auxiliary information. In the context of LST estimation, downscaling facilitates the derivation of fine-resolution temperature maps by establishing correlations between coarse-resolution thermal data and fine-scale spectral indices (Peng et al., 2021). Increasingly, machine learning algorithms have been deployed for LST downscaling because they can characterize nonlinear relationships between multidimensional land-surface variables and temperature observations.

The Random Forest algorithm demonstrates superior performance in LST prediction through its ensemble-based architecture, which minimizes overfitting while effectively handling multiple predictor variables (Bahi et al., 2025). RF integrates multiple decision trees via bootstrap aggregation to enhance predictive accuracy, rendering it well-suited for heterogeneous urban landscapes. Contemporary research has demonstrated that fusion of Landsat and Sentinel multispectral data utilizing RF algorithms substantially improves thermal mapping accuracy at local scales (Onačillová et al., 2022; Peng et al., 2021). Recent studies specifically employing RF-based downscaling approaches for LST refinement have validated the algorithm's effectiveness in urban thermal environment characterization (Bahi et al., 2025).

In tropical cities like Malang, where surface temperature gradients are influenced by elevation, vegetation cover, and land-use patterns, a high-resolution LST dataset is essential for understanding spatial heterogeneity. The ability to map temperature variations at 10 m resolution allows urban planners to identify critical heat-prone zones, assess the cooling function of green spaces, and evaluate the impact of urban expansion on local microclimates (Uhrin & Onačillová, 2025). Such information is vital for implementing climate adaptation strategies and promoting sustainable land management practices. Vegetation in tropical cities plays a fundamental role in mitigating urban heat through shading and evapotranspiration processes. High-resolution imagery has proven essential for assessing the spatial heterogeneity of urban vegetation, as diverse spectral signatures and three-dimensional structures have been observed in tropical settings (Martinuzzi et al., 2018). Recent work employing advanced remote sensing techniques at sub-meter resolutions supports the claim that urban green spaces not only reduce the urban heat island (UHI) intensity but also serve as indicators of socioeconomic variation across neighborhoods (Martinuzzi et al., 2018; Chen et al., 2022). Very high-resolution platforms facilitate the assessment of the cooling effects of green cover even when micro-scale spatial heterogeneity is significant, enabling a more robust integration of ecological and urban climatology models (Asmaryan et al., 2023).

Beyond documenting urban warming trends, high-resolution characterization of land surface temperature is fundamentally important for understanding the physical mechanisms governing urban climate dynamics. According to surface energy balance theory, LST is controlled by the partitioning of net radiation into sensible heat, latent heat, and ground heat flux, all of which are strongly modified by land-cover composition, surface moisture, and urban morphology (Voogt & Oke, 2003; Santamouris, 2020). Coarse-resolution thermal data obscure these interactions by spatially averaging heterogeneous surfaces, leading to underestimation of localized heat hotspots and limiting their applicability for urban-scale mitigation planning. Machine learning-based downscaling approaches, particularly Random Forest, provide a robust theoretical and practical framework for capturing nonlinear relationships between multispectral surface properties and thermal behavior, enabling the reconstruction of fine-scale LST patterns that align more closely with urban physical processes (Hengl et al., 2018; Peng et al., 2021). Conducting this research is therefore essential to bridge the gap between satellite-derived thermal observations and the spatial detail required for effective urban climate adaptation, especially in rapidly growing tropical cities like Malang, where complex interactions between urban expansion, vegetation loss, topography, and regional climate variability demand high-resolution thermal information for evidence-based planning and policy formulation.

The need for high-resolution LST datasets in tropical cities is underscored by the complex interplay of elevation, vegetation cover, and land-use patterns. Mapping surface temperature variations at a spatial resolution as fine as 10 m is critical for identifying localized heat-prone zones and tailoring climate adaptation strategies (Dimitrov et al., 2024). Studies have demonstrated that the integration of unmanned aerial systems (UAS) with remote sensing and geographic information systems (GIS) can produce the detailed thermal maps required to support urban planning decisions in data-scarce environments (Dimitrov et al., 2024). Similarly, advances in machine learning have led to process-informed neural architectures that predict urban surface temperatures with high accuracy, thereby enhancing both the precision and applicability of these datasets (Zang et al., 2023).

The objectives of this research are: (1) to integrate Landsat 8 and Sentinel-2 for enhancing the spatial resolution of LST in Malang City, (2) to assess the accuracy of the Random Forest downscaling approach, and (3) to analyze spatial and temporal variations of LST during 2019, 2022, and 2024. The outcomes are expected to provide a more robust understanding of urban thermal patterns, offering a scientific foundation for local climate adaptation strategies.

Method

Research Area

The research was conducted in Malang City, located at 112°06′–112°07′ E and 7°06′–8°02′ S. Malang is a city flanked by a mountain complex at 504.5 ± 48.3 masl with varied topography but slightly wavy relief. The research area is illustrated in Figure 1.

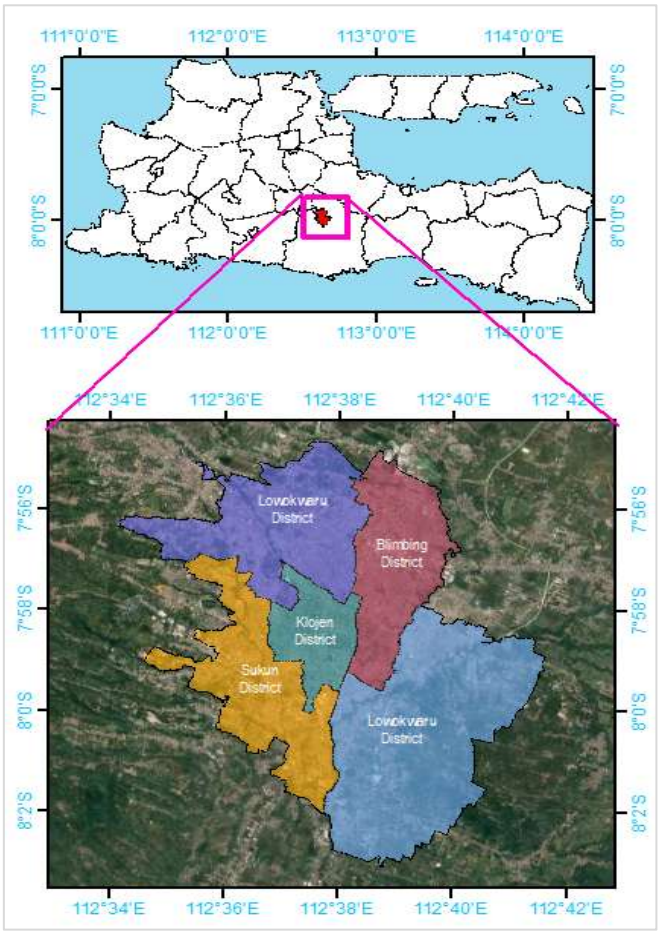

Figure 1. Research area

Materials

The following materials were used in this research: (a) Landsat 8 OLI/TIRS satellite imagery, path/row 118/066, freely downloaded from the USGS platform. (b) Sentinel-2 MSI satellite images, path 49MFM, freely downloaded from the Copernicus browser. These were chosen to have closely spaced acquisition dates to minimize the influence of emissivity changes on surface temperature calculations. (c) Satellite imagery was selected with a cloud cover range of less than 20%. The acquisition time details are shown in Table 1. (d) Infrared Thermometer Benetech GM900 for measuring

(e) Surface temperature. Land Cover for validation purposes.

Table 1. Selected Data Imagery Used in This Research

Satellite Imagery	Date Acquisition	Cloud Cover (%)
Landsat-8 OLI/TIRS	11 June 2019	6.98
	5 July 2022	13.82
	26 July 2024	6.98
Sentinel 2 MSI	10 June 2019	6.09
	9 July 2022	3.69
	23 July 2024	11.91

The research procedures are shown in Figure 2.

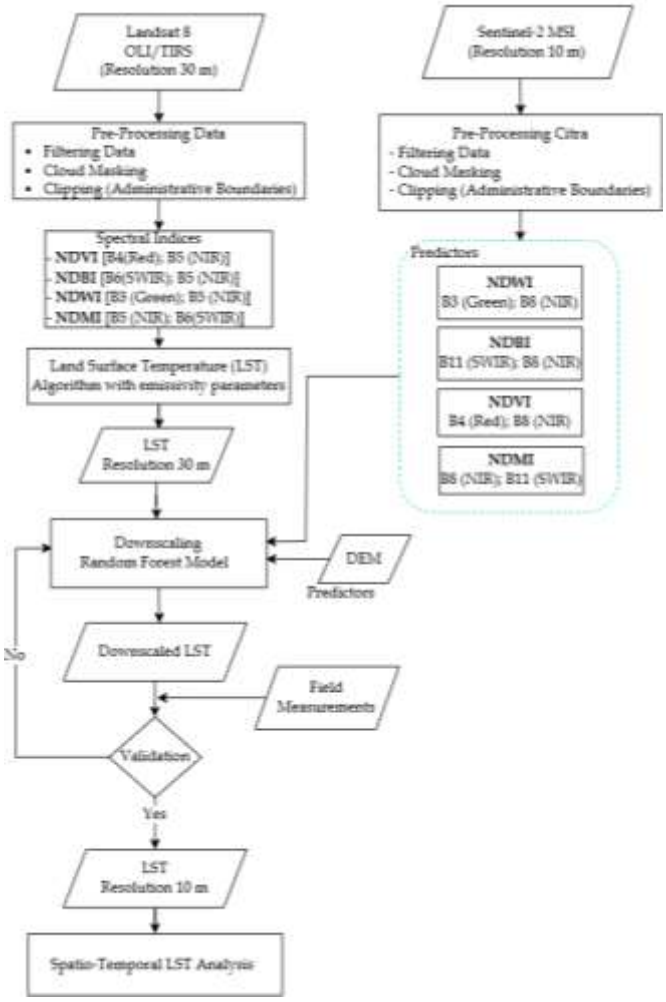

Figure 2. Research flow chart

Landsat 8 imagery, which includes 10 thermal infrared (TIRS) bands at 30 m spatial resolution, was used to derive LST using the mono-window and single-channel algorithms of Jiménez-Muñoz et al. (2003). The LST estimation followed the emissivity-based algorithm introduced by Artis et al. (1982), comprising the following steps: radiometric correction, brightness temperature conversion, NDVI calculation, vegetation proportion estimation, emissivity determination, and final LST computation. The Artis & Carnahan methodology has provided a foundational approach to LST estimation, numerous subsequent studies have addressed its inherent challenges. Emissivity retrieval methods exploiting VNIR and TIR data (Sobrino et al., 2008), refinements through NDVI and vegetation fraction modeling (Merlin et al., 2010), and advanced temperature/emissivity separation techniques (Liu et al., 2022; Cheng et al., 2008) have all enriched the field. Moreover, high-resolution studies (Yang et al., 2014; Song et al., 2015) emphasize the need for adapting the original framework to diverse and rapidly changing land surfaces. Such advancements not only improve the precision of LST estimates but also promote better-informed applications in environmental monitoring, resource management, and climate studies. The calculation method procedures are summarized below:

1. Radiometric correction is applied using the following equation:

$$L\lambda = ML \times Q_{ca} + AL \quad (1)$$

Where $L\lambda$ is TOA spectral radiance (Watts/m2 *srad*μm), ML is Radiance multiplicative band metadata, $Qcal$ is Digital Number band 10, AL is band-specific additive rescaling factor from the metadata.

2. Brightness temperature is then formulated as follows:

$$BT = \frac{K2}{Ln\left(\frac{K1}{L\lambda}\right)+1} \quad (2)$$

Where BT is the brightness temperature (in Kelvin), $L\lambda$ is the TOA spectral radiance (the corrected spectral radiance value), and K1 and K2 are calibration constants obtained from the metadata file. The values for K1 and K2 are 774.8853 and 1321.0789, respectively.

3. The brightness temperature values were converted from Kelvin to Celsius:

$$BT_{celcius} = BT - 273{,}15 \quad (3)$$

4. The NDVI value was calculated (Rousse et al., 1973).

$$NDVI = \frac{NIR-RED}{NIR+RED} \quad (4)$$

5. Which was subsequently used to calculate the proportion of vegetation (P_v) using equation (5).

$$P_v = \left(\frac{NDVI - NDVI_{min}}{NDVI_{max} - NDVI_{min}}\right)^2 \quad (5)$$

6. Emissivity (ε) was calculated using equation (6).

$$\varepsilon = 0.0004\ Pv + 0.986 \quad (6)$$

7. The resulting Emissivity is then entered into equation (7) to find LST.

$$LST = \frac{B_T}{1+\left(\lambda . \frac{B_T}{\rho}\right) \ln \varepsilon} \quad (7)$$

Where ρ = (h.c)/σ. The formulation contains several parameters, which means the wavelength of the emitted radiance, = 1,438 x 10-2 mK, for h = Planck's constant (6,626 x 10-34 Js), C represents the speed of light (2,998 x 108 m/s), and σ refers to Boltzmann's Constant (14388).

Common indices used to enhance LST resolution include NDVI, built-up areas (NDBI), water bodies (NDWI), and surface moisture (NDMI), all processed in QGIS. The Red, Green, Near-Infrared (NIR), and Shortwave Infrared (SWIR) bands from Landsat 8 and Sentinel-2 were used to calculate related spectral indices (Gao, 1996; Rousse et al., 1973; Zha et al., 2003). The equations for each index are presented in Table 2.

Table 2. Equation Spectral Indices

Equation		Reference
$NDBI = \frac{SWIR-NIR}{SWIR+NIR}$	(8)	(Zha et al., 2003)
$NDWI = \frac{Green-NIR}{Green+NIR}$	(9)	(Gao, 1996)
$NDMI = \frac{NIR-SWIR}{NIR+SWIR}$	(10)	(Gao, 1996)

All common indices, DEM, and low-resolution LST were utilized as inputs for the downscaling process. The LST downscaling was performed using the QGIS plugin named 'Downscale Anything with Random Forest', which employs the Random Forest algorithm integrated with Google Earth Engine (GEE). The downscaling procedure of LST using the Random Forest approach is illustrated in Figure 3.

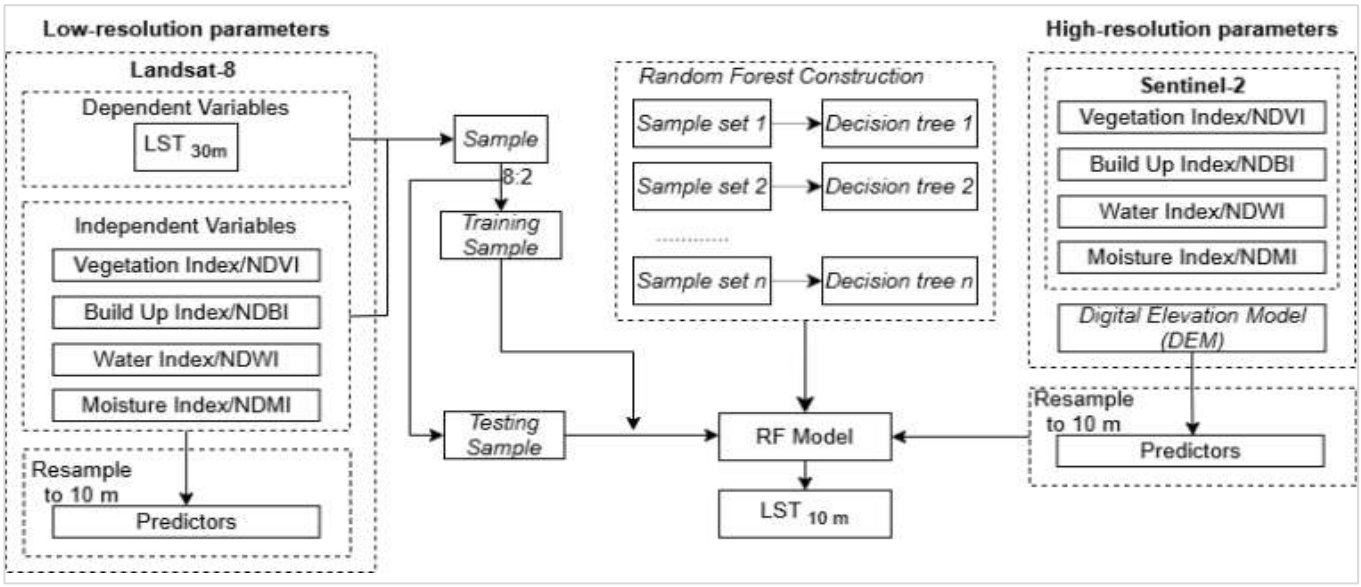

Figure 3. Flow chart of downscaling LST based on random forest

The RF model was constructed using multiple decision trees trained on 80% of the data and validated on 20% to reduce overfitting (Hengl et al., 2018; Kuhn & Johnson, 2019). Predictor variables with 10 m spatial resolution were used to estimate high-resolution LST, capturing microscale variations in surface temperature. Model performance, evaluated using R^2 and RMSE (Peng et al., 2021; Roy et al., 2025). A lower RMSE indicates higher agreement between observed and predicted LST. Since the RF model does not fully represent the complete LST distribution, a residual correction was applied.

Validation Data

Field surface temperature measurements for LST downscaling validation were conducted using a Thermal Infrared thermometer. The methodology adopted follows Chiueh et al. (2021), where the emissivity value for each surface material was applied as specified in that study. Sampling sites were selected based on land-use classifications derived from the Malang City Urban Planning Land Cover Map (1:25,000 scale); details are provided in Table 3, and their spatial distribution is shown in Figure 4. To ensure temporal synchronization with satellite data acquisition, aligning with the Landsat 8 and Sentinel-2 overpass time. This

standardized protocol is consistent with other LST validation studies Chiueh et al. (2021).

Table 3. Number of Points of Validation in the Research Area

Land Use	Samples
Water body point	15
Building and road point	28
Upland crop point	18
Green space point	22
Paddy point	28
Bare land point	20
Total	131

Figure 4. Distribution LST observations

A linear regression analysis was applied to assess the relationship between the processed LST and observed LST. The regression results were further used to calculate RMSE, which indicated the level of bias between the datasets (Galve et al., 2022). The RMSE is calculated using the following equation:

$$RMSE = \sqrt{\frac{1}{n}\sum_{i=1}^{n}(P_i - O_i)^2} \quad (11)$$

Where P_i is for LST Processed and O_i is for LST Observation.

Data Analysis

This study employed integrated spatial, temporal, statistical, and descriptive analyses to examine LST dynamics in Malang City. Spatial analysis quantified and visualized thermal distribution patterns to identify urban heat anomalies and their impact within administrative boundaries (Rakuasa et al., 2023), while temporal analysis assessed the effects of urbanization on thermal intensity over five years. Statistical and descriptive methods synthesized multi-source remote sensing data, using descriptive statistics (mean, minimum, maximum, and standard deviation).

Result and Discussion

Integration of Landsat 8 and Sentinel-2 for Enhanced LST Spatial Resolution through Random Forest

The integration of Landsat 8 OLI/TIRS and Sentinel-2 MSI data effectively enhanced the spatial resolution of LST from 30 m to 10 m in Malang City. The Random Forest-based downscaling approach produced high-detail surface temperature maps capable of identifying microscale thermal variations within complex urban environments. Figure 5 illustrates a comparison for 2019, showing the original 30 m LST (Fig. 5A) and the downscaled 10 m LST, which reveals a clearly improved (sharpened) thermal pattern (Fig. 5B).

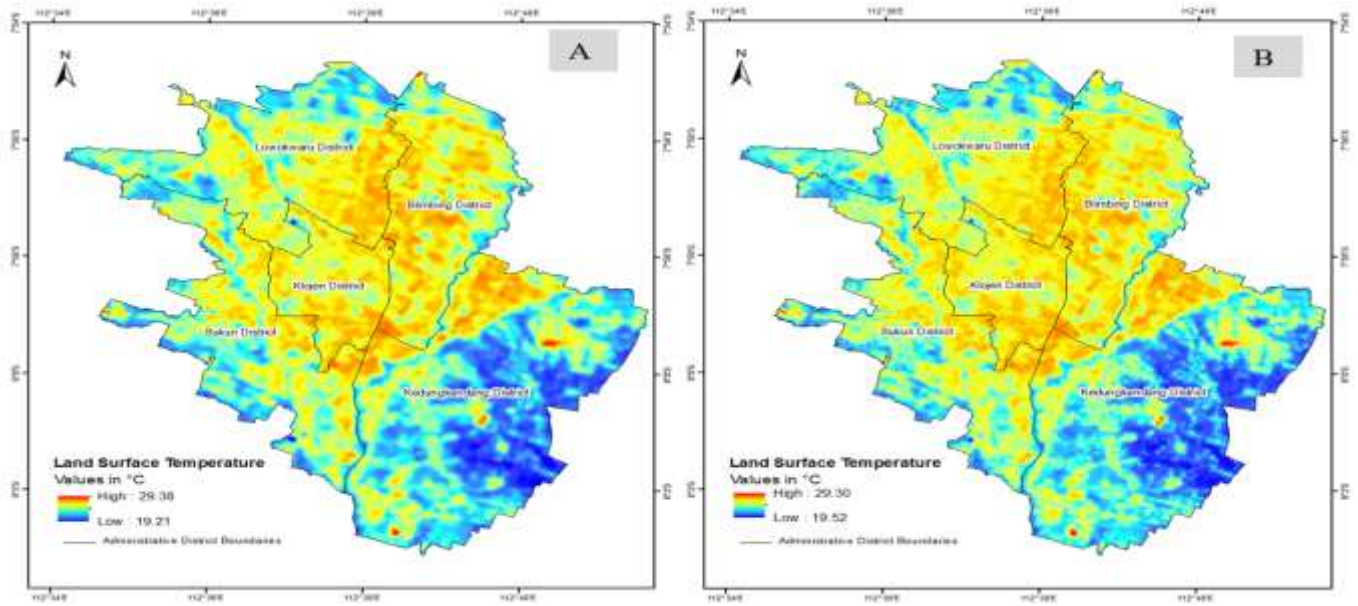

Figure 5. (A) Coarse LST derived from Landsat-8 in spatial resolution of 30 m, (B) downscaled finer LST in spatial resolution of 10 m, for the study area of the Malang city in 2019

Model evaluation across the three observation years showed that 2019 achieved high accuracy (R^2 = 0.8374, RMSE = 0.6485°C, OOB = 0.8360), while 2022 recorded improved accuracy (R^2 = 0.8468, RMSE = 0.5903°C, OOB = 0.8441). In 2024, performance slightly declined but remained strong (R^2 = 0.7675, RMSE = 0.7116°C, MAE = 0.5394°C, OOB = 0.7634), reflecting the growing complexity of urban surface characteristics, which challenged model generalization (Roy et al., 2025; Uhrin & Onačillová, 2025). Despite this, the R^2 value of 0.7675 still indicates strong model reliability, explaining more than 76% of LST variability.

Residual distribution analysis further confirmed model validity, with histograms for 2019, 2022, and 2024 showing symmetric, bell-shaped curves centered near zero, indicating unbiased predictions with minimal net error across all periods shown in Figure 6.

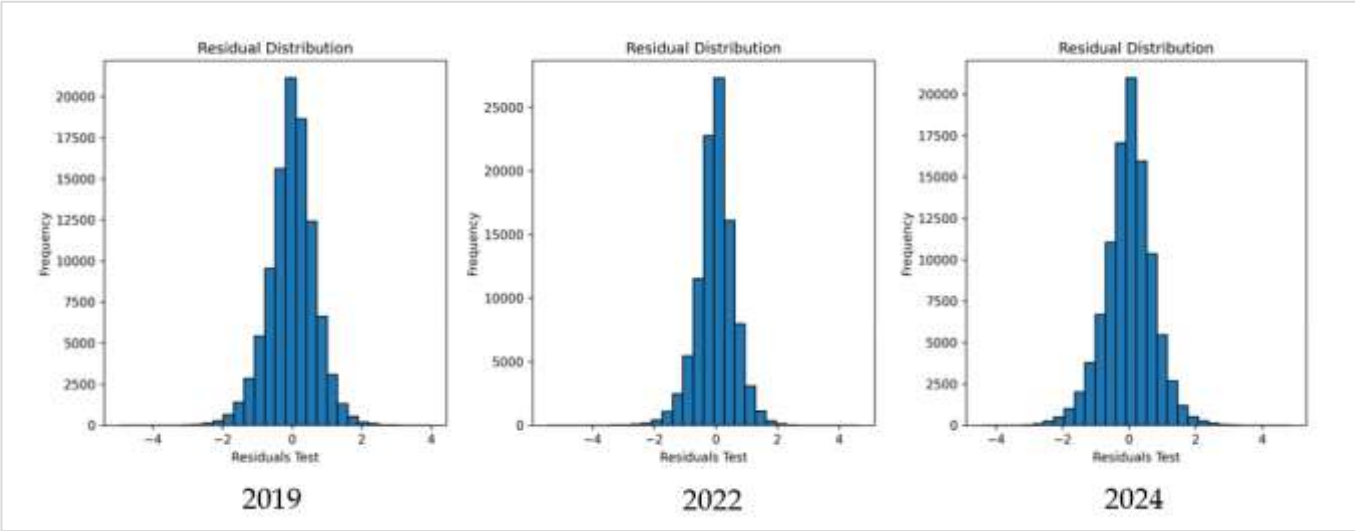

Figure 6. Residual distribution on each period

The scatter plot in Figure 7 further supports this result. Validation using 131 in-situ measurement points demonstrates a moderate-to-strong correlation, yielding a Pearson's correlation coefficient (r) of 0.722 (R^2 = 0.5214) and an RMSE of 4.63°C. This integration approach aligns with recent advancements in urban remote sensing that emphasize the importance of multisensor data fusion to improve spatial accuracy. The results also confirm robust model reliability, supported by normal error distribution and consistent unbiased residual patterns (Bahi et al., 2025).

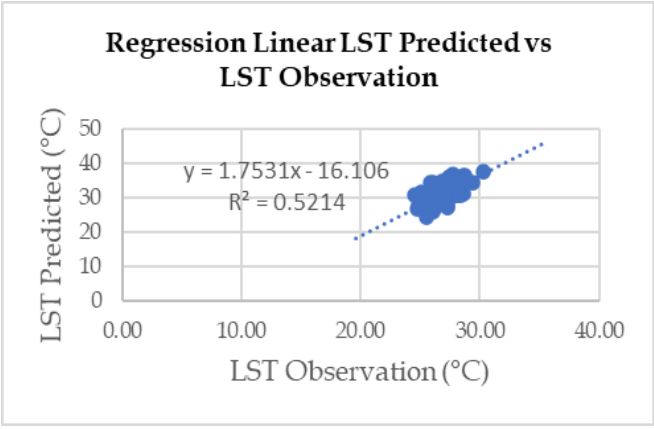

Figure 7. Regression linear LST predicted vs LST observation

Spatial-temporal variations of LST during 2019, 2022, and 2024

Analysis of spatial and temporal LST variations in Malang City identifies significant warming from 2019 to 2024. Downscaled 10 m LST data revealed detailed thermal distributions, highlighting substantial spatial heterogeneity and accelerated temporal changes, especially during 2022–2024. City-wide statistics are shown in Table 4, district-level statistics in Table 5, and the spatial distribution is visually represented in Figure 8.

Table 4. LST Malang City 2019-2024

Year	Max (°C)	Mean (°C)	Min (°C)	Std.
11 June 2019	29.30	25.00	19.52	1.12
5 July 2022	28.61	25.28	17.65	1.11
26 July 2024	32.12	27.47	22.46	1.05

In 2019, the city-wide mean LST was 25.00°C, with a range from 19.52°C to 29.30°C (Std = 1.12°C). As detailed in Table 5, Klojen District, the commercial core, was the hottest (mean 25.90°C). It was followed by Blimbing (25.60°C), Lowokwaru (25.01°C), and Sukun (24.79°C). Kedungkandang was the coolest district (23.71°C), reflecting its higher vegetation coverage (Sejati et al., 2019). Notably, Kedungkandang also had

the highest Std 1.59°C, indicating significant intra-district heterogeneity.

By 2022, the city-wide mean LST increased moderately to 25.28°C (0.28°C higher than 2019). The spatial ranking remained consistent: Klojen recorded the highest mean LST (26.24°C), followed by Blimbing (25.91°C), Sukun (25.22°C), Lowokwaru (24.71°C), and Kedungkandang (24.30°C). Despite the modest city-wide mean increase, differential warming existed. Blimbing (0.31°C rise) and Klojen (0.34°C increase) warmed significantly. In contrast, Lowokwaru experienced slight cooling (a decrease of 0.30°C). This divergence is linked to heterogeneous land-use conversion and differential green-space policies (Hidayati et al., 2019; Tesfamariam et al., 2023).

Table 5. LST 2019, 2022, 2024 in Celsius per District

District	2019				2022				2024			
	Max	Mean	Min	Std.	Max	Mean	Min	Std.	Max	Mean	Min	Std.
Blimbing	28.40	25.60	21.69	0.97	28.24	25.91	19.53	0.96	30.63	28.02	23.15	1.01
Kedungkandang	29.30	23.71	20.34	1.59	28.50	24.30	19.18	1.46	31.77	26.58	22.46	1.46
Klojen	27.34	25.90	20.70	0.67	28.29	26.24	22.56	0.76	30.08	28.23	24.68	0.63
Lowokwaru	27.55	25.01	20.97	1.17	27.65	24.71	17.72	1.31	31.07	27.32	23.69	1.05
Sukun	27.96	24.79	19.52	1.20	28.73	25.22	21.22	1.09	32.12	27.19	23.49	1.12

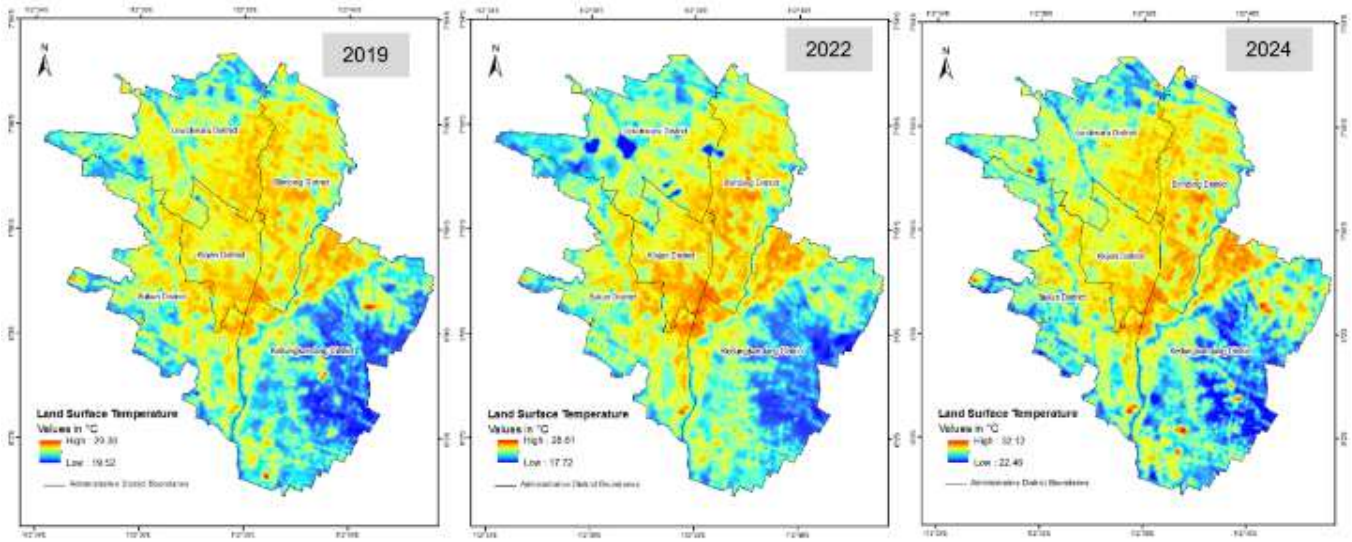

Figure 8. LST spatial distribution 2019, 2022, 2024

The 2024 period exhibited dramatic, accelerated warming. The city-wide mean LST increased sharply to 27.47°C (2.19°C above 2022 and 2.47°C above 2019), representing a 2019–2024 warming rate of 0.508°C/year. The maximum LST reached an observational high of 32.12°C. All five districts warmed substantially from 2022 to 2024 (illustrated in Figure 9), led by Lowokwaru (increase of 2.61°C) and Kedungkandang (increase of 2.28°C). Although Klojen remained the hottest (28.23°C), the inter-district thermal range narrowed (1.65°C in 2024 versus 2.19°C in 2019), suggesting thermal homogenization across the city (Chen et al., 2022; Ding et al., 2025).

The intra-district temperature range (Maximum-Minimum) highlights internal thermal heterogeneity. Kedungkandang consistently displayed the widest range (8.96°C in 2019; 9.31°C in 2024), indicating the coexistence of developed and preserved lands. Conversely, Klojen's range narrowed (6.64°C in 2019 to 5.40°C in 2024), showing thermal homogeneity in the fully developed urbanized core.

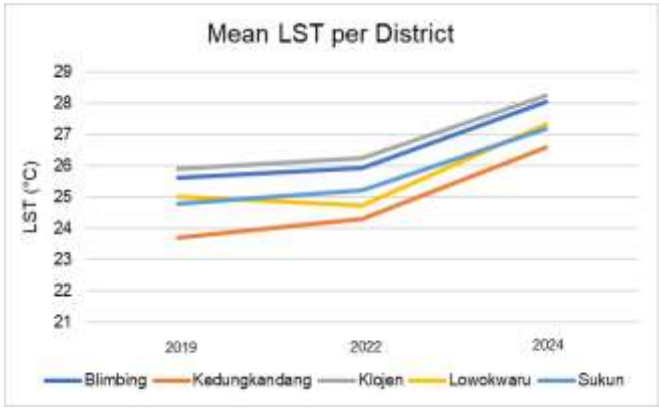

Figure 9. Tren spasiotemporal LST 2019-2024

Temporal analysis reveals a distinct two-phase warming pattern that fundamentally changed urban

thermal dynamics over the five-year period. Phase 1 (2019–2022) exhibited a moderate increase of 0.28°C city-wide, corresponding to a warming rate of 0.14°C per year. In sharp contrast, Phase 2 (2022–2024) demonstrated a dramatic acceleration of 2.19°C city-wide, corresponding to a rate of 1.10°C per year—approximately seven times faster than Phase 1. This nonlinear progression represents a critical acceleration in urban thermal intensification. The accelerated warming during 2022–2024 is attributed to the combined effects of rapid land conversion, intensive post-pandemic economic development (Purwantara & Ashari, 2025), and amplification by regional climate oscillations.

The most critical LST increases occurred when local urban development drivers interacted with regional climate forcing. This period notably coincided with the 2023 El Niño event, one of the strongest on record, and a concurrent positive Indian Ocean Dipole (IOD). These phenomena are known to increase land surface temperatures across Indonesia by reducing cloud cover and enhancing solar radiation (Berliani et al., 2025; Eboy & Kemarau, 2023). Urban expansion, which converts permeable vegetation to impermeable surfaces, reduces evaporative cooling capacity; this effect was severely amplified by the reduced atmospheric moisture associated with the ENSO and IOD phases. Malang's total 2.54°C warming over five years, a rate comparable to or greater than other Indonesian cities (Apriana & Syahrani, 2022), aligns with findings in Semarang where similar urban expansion and vegetation decline led to 2-5°C temperature increases (Sejati et al., 2019).

These findings have substantial implications for urban planning, confirming that urban form characteristics like building density are strong drivers of LST, as seen in Klojen, the warmest and highest-density district (Ding et al., 2025). The analysis mandates targeted, spatially-specific interventions: persistent hotspots (Klojen) require retrofitting with cool roofs or green walls, while rapidly warming transitional zones (Kedungkandang, Lowokwaru) require proactive planning with conservation buffers and mandatory green space ratios (Chen et al., 2022; Tesfamariam et al., 2023). Furthermore, the declining city-wide thermal heterogeneity (Std decreasing from 1.51°C to 1.34°C) indicates that Urban Heat Island (UHI) effects are becoming widespread, necessitating immediate, city-wide mitigation strategies (Hasyim et al., 2025; Sejati et al., 2019).

Conclusion

This study confirms the effectiveness of the proposed Random Forest-based downscaling approach for enhancing LST spatial resolution from 30 m to 10 m using Landsat 8 and Sentinel-2 data in Malang City. The model demonstrated strong accuracy and reliability (R^2 = 0.7675, RMSE = 0.7116°C) and consistent field validation (r = 0.722, RMSE = 4.63°C). Residual analysis indicated unbiased predictions across all observation periods. The consistently high model performance across multiple years, with R^2 values consistently exceeding 0.76, confirms the reliability of this methodology for capturing complex urban thermal heterogeneity that coarser satellite products fail to resolve. The systematic validation against ground-truthed measurements provides empirical confidence in the downscaled LST estimates, thereby establishing this framework as a transferable solution applicable to other tropical urban contexts. Spatio-temporal analysis revealed a clear warming trend of 0.62°C per year from 2019 to 2024, accelerating to 1.10°C per year between 2022 and 2024. Klojen District remained the primary urban hotspot, while Kedungkandang experienced the fastest warming due to rapid suburban expansion. The decrease in city-wide temperature variability suggests intensifying urban heat island effects Overall, the developed method provides accurate, high-resolution thermal information essential for designing targeted urban heat mitigation and climate adaptation strategies in rapidly growing tropical cities. While the model demonstrated strong performance, its predictive ability decreased in 2024 due to rapid urban transformation and limited field validation, underscoring the need to retrain on multi-temporal data and expand ground measurement coverage. Future studies should incorporate broader climatic factors and multi-city comparisons to strengthen reliability and establish this method as a practical foundation for urban heat mitigation and adaptive planning strategies.

Acknowledgments
Thank you to the Ministry of National Development Planning/National Development Planning Agency (Bappenas) and the Malang City Government for the cost-sharing scholarship. We also thank all parties who have supported the implementation of this research.

Author Contributions
All authors have read and agreed to the published version of the manuscript.

Funding
This research was funded by the Ministry of National Development Planning/National Development Planning Agency (Bappenas) and the Malang City Government.

Conflicts of Interest
All authors declare that they have no conflict of interest.

References

Apriana, M., & Syahrani, E. (2022). Land Surface Temperature and its Relationship to Population Density. *Journal of Applied Geospatial Information*, *6*(1), 569–575. https://doi.org/10.30871/jagi.v6i1.1936

Artis, D. A., & Carnahan, W. H. (1982). Survey of emissivity variability in thermography of urban areas. *Remote Sensing of Environment*, *12*(4), 313–329. https://doi.org/10.1016/0034-4257(82)90043-8

Asmaryan, S., Muradyan, V., Medvedev, A., Avetisyan, R., Hovsepyan, A., Khlghatyan, A., & Dell'Acqua, F. (2023). Exploring Very High-Resolution Remote Sensing for Assessing Land Surface Temperature of Different Urban Land Cover Patterns. *The International Archives of the Photogrammetry, Remote Sensing and Spatial Information Sciences, XLVIII-1/W2-2023,* 1847-1852. https://doi.org/10.5194/isprs-archives-xlviii-1-w2-2023-1847-2023

Bahi, H., Bounoua, L., Sabri, A., Bannari, A., Malah, A., & Rhinane, H. (2025). A new thermal fusion method to downscale Land Surface Temperature to finer spatial resolution using Sentinel-MSI and Landsat-OLI/TIRS imagery. *Remote Sensing Applications: Society and Environment*, *37*, 101519. https://doi.org/10.1016/j.rsase.2025.101519

Berliani, R., Rosenberg, A., & Prayoga, D. (2025). Identifikasi suhu permukaan laut pada saat El Niño dan IOD positif 2023 di Perairan Barat Sumatera. *Jurnal Kelautan*, *9*(1), 45–58. https://doi.org/10.21107/jk.v18i1.29100.

Chen, S., Yang, Y., Deng, F., Zhang, Y., Liu, D., Liu, C., & Gao, Z. (2022). A high-resolution monitoring approach of canopy urban heat island using a random forest model and multi-platform observations. *Atmospheric Measurement Techniques, 15*(3), 735-756. https://doi.org/10.5194/amt-15-735-2022.

Chen, Y., Shan, B., & Yu, X. (2022). Study on the spatial heterogeneity of urban heat islands and influencing factors. *Building and Environment*, *208*(108604). https://doi.org/10.1016/j.buildenv.2021.108596

Cheng, J., Liu, Q., Li, X., Xiao, Q., Liu, Q., & Du, Y. (2008). Correlation-based temperature and emissivity separation algorithm. *Science in China Series D: Earth Sciences, 51*(3), 357-369. https://doi.org/10.1007/s11430-008-0022-7

Chiueh, Y.-W., Tan, C.-H., & Hsu, H.-Y. (2021). The Value of a Decrease in Temperature by One Degree Celsius of the Regional Microclimate—The Cooling Effect of the Paddy Field. *Atmosphere*, *12*(3), 353. https://doi.org/10.3390/atmos12030353

Dimitrov, S., Iliev, M., Borisova, B., Semerdzhieva, L., & Petrov, S. (2024). A Methodological Framework for High-Resolution Surface Urban Heat Island Mapping: Integration of UAS Remote Sensing, GIS, and the Local Climate Zoning Concept. *Remote Sensing, 16*(21), 4007. https://doi.org/10.3390/rs16214007

Ding, L., Xiao, X., & Wang, H. (2025). *Temporal and spatial variations of urban surface temperature and correlation study of influencing factors*. https://doi.org/10.1038/s41598-025-85146-4

Eboy, O. V., & Kemarau, R. A. (2023). Analysis of Extreme Heat Land Surface Temperature at a Tropical City (1988-2022): A Study on the Variability of Hot Spot during El Niño Southern Oscillation (ENSO). *Science & Technology Indonesia*, *8*(3), 388–396. https://doi.org/10.26554/sti.2023.8.3.388-396

Galve, J. M., Sánchez, J. M., García-Santos, V., González-Piqueras, J., Calera, A., & Villodre, J. (2022). Assessment of Land Surface Temperature Estimates from Landsat 8-TIRS in A High-Contrast Semiarid Agroecosystem. Algorithms Intercomparison. *Remote Sensing*, *14*(8), 1843. https://doi.org/10.3390/rs14081843

Gao, B. (1996). NDWI—A normalized difference water index for remote sensing of vegetation liquid water from space. *Remote Sensing of Environment*, *58*(3), 257–266. https://doi.org/10.1016/S0034-4257(96)00067-3

Hasyim, A. W., Sukojo, B. M., Anggraini, I. A., Fatahillah, E. R., & Isdianto, A. (2025). Urban Heat Island Effect and Sustainable Planning: Analysis of Land Surface Temperature and Vegetation in Malang City. *International Journal of Sustainable Development and Planning*, *20*(2), 683–697. https://doi.org/10.18280/ijsdp.200218

Hengl, T., Nussbaum, M., Wright, M. N., Heuvelink, G. B. M., & Gräler, B. (2018). Random forest as a generic framework for predictive modeling of spatial and spatio-temporal variables. *PeerJ*, *6*, e5518. https://doi.org/10.7717/peerj.5518

Hidayati, I. N., Suharyadi, R., & Danoedoro, P. (2019). Environmental quality assessment of urban ecology based on spatial heterogeneity and remote sensing imagery. *KnE Social Sciences*, *13*(1), 363–379. https://doi.org/10.18502/kss.v3i21.4981

Irfeey, A. M. M., Chau, H.-W., Sumaiya, M. M. F., Wai, C. Y., Muttil, N., & Jamei, E. (2023). Sustainable Mitigation Strategies for Urban Heat Island Effects in Urban Areas. *Sustainability*, *15*(14), 10767. https://doi.org/10.3390/su151410767

Isdianto, A., Hasyim, A. W., Sukojo, B. M., Alimuddin,

I., Anggraini, I. A., & Fatahillah, E. R. (2025). Integrating Urban Design with Natural Dynamics: Enhancing Ecological Resilience in Malang City over a Decade. *International Journal of Sustainable Development and Planning*, *20*(3), 1061–1075. https://doi.org/10.18280/ijsdp.200313

Jiménez-Muñoz, J. C., & Sobrino, J. A. (2003). A generalized single-channel method for retrieving land surface temperature from remote sensing data. *Journal of Geophysical Research: Atmospheres*, *108*(D22). https://doi.org/10.1029/2003JD003480

Kuhn, M., & Johnson, K. (2019). *Feature Engineering and Selection*. Chapman and Hall/CRC. https://doi.org/10.1201/9781315108230

Liu, P., Huo, H., Guo, L., Leng, P., & He, L. (2022). Temperature/Emissivity Separation of Typical Grassland of Northwestern China Based on Hyper-CAM and Its Potential for Grassland Drought Monitoring. *Remote Sensing*, *14*(19), 4809. https://doi.org/10.3390/rs14194809

Li, J., Yang, Z., Zhao, X., Li, Y., Huang, X., Chen, Y., & Shi, F. (2024). Study of the Correlation between the Urban Wind–Heat Environment and Urban Development Elements in High-Density Urban Areas: A Case Study of Central Shanghai. *Buildings*, *14*(2), 315. https://doi.org/10.3390/buildings14020315

Martinuzzi, S., Ramos-González, O. M., Muñoz-Erickson, T. A., Locke, D. H., Lugo, A. E., & Radeloff, V. C. (2018). Vegetation cover in relation to socioeconomic factors in a tropical city assessed from sub-meter resolution imagery. *Ecological Applications,* *28*(3), 681-693. https://doi.org/10.1002/eap.1673.

Merlin, O., Duchemin, B., Hagolle, O., Jacob, F., Coudert, B., Chehbouni, G., & Kerr, Y. H. (2010). Disaggregation of MODIS surface temperature over an agricultural area using a time series of Formosat-2 images. *Remote Sensing of Environment,* *114*(11), 2500-2512. https://doi.org/10.1016/j.rse.2010.05.025

Onačillová, K., Gallay, M., Paluba, D., Péliová, A., Tokarčík, O., & Laubertová, D. (2022). Combining Landsat 8 and Sentinel-2 Data in Google Earth Engine to Derive Higher Resolution Land Surface Temperature Maps in Urban Environment. *Remote Sensing*, *14*(16), 4076. https://doi.org/10.3390/rs14164076

Peng, Yuan, X., Gao, W., Wang, R., & Chen, W. (2021). Assessment of urban cooling effect based on downscaled land surface temperature: A case study for Fukuoka, Japan. *Urban Climate*, *36*, 100790. https://doi.org/10.1016/j.uclim.2021.100790

Purwantara, S., & Ashari, A. (2025). Spatio-temporal variability of urban surface temperature during COVID-19 pandemic: A study from some selected cities in Indonesia and Singapore. *Jurnal Wilayah Dan Lingkungan*, *12*(3), 279–292. https://doi.org/https://doi.org/10.14710/jwl.12.3.279-292

Rakuasa, H., Sihasale, D. A., & Latue, P. C. (2023). Spatial pattern of changes in land surface temperature of seram island based on google earth engine cloud computing. *International Journal of Basic and Applied Science*, *12*(1), 1–9. https://doi.org/10.35335/ijobas.v12i1.172

Rousse, J. W., Haas, R. H., Schell, J., & Deering, D. W. (1973). Monitoring vegetation systems in the Great Plains with ERTS. *Third Earth Resources Technology Satellite-1 Symposium (NASA SP-351)*, 309–317. Retrieved from https://ntrs.nasa.gov/citations/19740022614

Roy, D., Das, B., Singh, P., Santra, P., Deb, S., Bhattacharya, B. K., Govind, A., Jatav, R., Sethi, D., Ghosh, T., Mukherjee, J., Sehgal, V. K., Jha, P. K., Goroshi, S., Prasad, P. V. V., & Chakraborty, D. (2025). Assessing the accuracy of multi-model approaches for downscaling land surface temperature across diverse agroclimatic zones. *Scientific Reports*, *15*(1), 10824. https://doi.org/10.1038/s41598-025-92135-0

Santamouris, M. (2020). Recent Progress on Urban Overheating and Heat Island Research. Integrated Assessment of The Energy, Environmental, Vulnerability and Health Impact. Synergies with The Global Climate Change. *Energy and Buildings*, *207*, 109482. https://doi.org/10.1016/j.enbuild.2019.109482

Sejati, A. W., Buchori, I., & Rudiarto, I. (2019). The spatio-temporal trends of urban growth and surface urban heat islands over two decades in the Semarang Metropolitan Region. *Sustainable Cities and Society*, *46*. https://doi.org/10.1016/j.scs.2019.101432

Sobrino, J. A., Jiménez-Muñoz, J. C., Sòria, G., Romaguera, M., Guanter, L., Moreno, J., & Martínez, P. (2008). Land Surface Emissivity Retrieval From Different VNIR and TIR Sensors. *IEEE Transactions on Geoscience and Remote Sensing,* *46*(2), 316-327. https://doi.org/10.1109/tgrs.2007.904834

Song, L., Liu, S., Kustas, W. P., Zhou, J., & Ma, Y. (2015). Using the Surface Temperature-Albedo Space to Separate Regional Soil and Vegetation Temperatures from ASTER Data. *Remote Sensing,* *7*(5), 5828-5848. https://doi.org/10.3390/rs70505828

Tesfamariam, S., Govindu, V., & Uncha, A. (2023). Spatio-temporal analysis of urban heat island

(UHI) and its effect on urban ecology: The case of Mekelle city, Northern Ethiopia. *Heliyon*, *9*(2). https://doi.org/10.1016/j.heliyon.2023.e13098

Uhrin, A., & Onačillová, K. (2025). Spatiotemporal analysis of land surface temperature and land cover changes in Prešov city using downscaling approach and machine learning algorithms. *Environmental Monitoring and Assessment*, *197*(2), 126. https://doi.org/10.1007/s10661-024-13598-8

Voogt, J. ., & Oke, T. (2003). Thermal remote sensing of urban climates. *Remote Sensing of Environment*, *86*(3), 370–384. https://doi.org/10.1016/S0034-4257(03)00079-8

Yang, L., Cao, Y., Zhu, X., Zeng, S., Yang, G., He, J., & Yang, X. (2014). Land surface temperature retrieval for arid regions based on Landsat-8 TIRS data: a case study in Shihezi, Northwest China. *Journal of Arid Land,* *6*(6), 704-716. https://doi.org/10.1007/s40333-014-0071-z

Zahro, H., Sobirin, S., & Wibowo, A. (2018). Variasi spasiotemporal urban heat island di kawasan perkotaan Yogjakarta tahun 2015-2017. *Jurnal Geografi Lingkungan Tropik*, *2*(1). https://doi.org/10.7454/jglitrop.v2i1.35.

Zang, Y., Huang, G., Liu, W., Chen, L., Wu, D., Wang, C., & Li, J. (2023). Deepurbanmodeller (Dum): A Process-Informed Neural Architecture For High-Precision Urban Surface Temperature Prediction. *The International Archives of the Photogrammetry Remote Sensing and Spatial Information Sciences, XLVIII-1/W2-2023,* 71-76. https://doi.org/10.5194/isprs-archives-xlviii-1-w2-2023-71-2023.

Zha, Y., Gao, J., & Ni, S. (2003). Use of normalized difference built-up index in automatically mapping urban areas from TM imagery. *International Journal of Remote Sensing*, *24*(3), 583–594. https://doi.org/10.1080/01431160304987